CHAPTER-2

CHEMICAL REACTION AND RADIATION EFFECTS ON UNSTEADY MHD NATURAL CONVECTION FLOW OF A ROTATING FLUID PAST A VERTICAL POROUS FLAT PLATE IN THE PRESENCE OF VISCOUS DISSIPATION

2.1 INTRODUCTION

The flow of incompressible Boussinesq fluid in the presence of rotation has application in space science and engineering fluid dynamics. The effects of Hall current on hydro-magnetic free convection with mass transfer in a rotating fluid was studied by Agarwal et al. [1].Bestman and Adjepong [4] studied unsteady hydro-magnetic free convection flow with radiative heat transfer in a rotating fluid. Radiation effects on the MHD mixed free-fixed convection flow past a semi-infinite moving vertical plate for high temperature differences was studied by Azzam [2]. Bestman [3] studied free convection heat transfer to unsteady radiating non-Newtonian MHD flow past a vertical porous plate. Chamkha [5] studied thermal radiation and buoyancy effects on hydro-magnetic flow over an accelerating permeable surface with heat source or sink. Chamkha [6] investigated unsteady convective heat and mass transfer past a semi-infinite permeable moving plate with heat absorption where it was found that increase in solutal Grashoff number enhanced the concentration buoyancy effects leading to an increase in the velocity. Cookey et al. [7] studied influence of viscous dissipation and radiation on unsteady MHD free convection flow past an infinite heated vertical plate in a porous medium with time dependent suction. Elbarbary and Elgazery [8] studied effect of variable viscosity on magnetic micro-polar fluid flow with radiation by the Chebyshev finite difference method. Gireesh Kumar et al. [9] studied effects of the chemical reaction and mass transfer on MHD unsteady free convection flow past an infinite vertical plate with constant suction and heat sink. Helmy [10] focused on MHD flow in a micro-polar fluid. In another recent study Ibrahmin et al. [11] investigated unsteady magneto-hydrodynamic micro-polar fluid flow and heat transfer over a vertical porous plate through a porous medium in the presence of thermal and mass diffusion with a

constant heat source. Jha [12] studied MHD free-convection and mass transfer flow through a porous medium but did not consider the effect of radiation which is of great relevance to astrophysical and cosmic studies. Kandasamy et al. [13] investigated the effects of chemical reaction, heat and mass transfer along a wedge with heat source and convection in the presence of suction or injection. Kesavaiah et al. [14] studied effects of the chemical reaction and radiation absorption on an unsteady MHD convective heat and mass transfer flow past a semi-infinite vertical permeable moving plate embedded in a porous medium with heat source and suction. Kim [15] studied unsteady MHD convective heat transfer past a semi-infinite vertical porous moving plate with variable suction. Muthucumaraswamy and Ganesan [16] studied natural convection on a moving isothermal vertical plate with chemical reaction. Ogulu and Cookey [17] studied MHD free-convection and mass transfer flow with radiative heat transfer. Heat transfer to unsteady magneto-hydrodynamic flow past an infinite moving vertical plate with variable suction was the focus of an earlier study reported by Ogulu and Prakash [18], where it was shown that increasing the plate velocity has the effect of increasing the flow velocity with this increase been more pronounced for higher values of the free convection. Prakash et al. [19] studied MHD free convection and mass transfer flow of a micro-polar thermally radiating and reacting fluid with time dependent suction. Non-Darcian forced convection heat transfer over a flat plate in porous medium with variable viscosity and variable Prandtl number was studied by Pantokratoras [20]. Effects of the chemical reaction and radiation absorption on free convective flow through porous medium with variable suction in the presence of uniform magnetic field were studied by sudheer babu and satyanarayana [21].

The main objective of the present investigation is to study the effects of radiation and chemical reaction on unsteady MHD natural convection flow of a rotating fluid past

a vertical porous flat plate in the presence of viscous dissipation. The equations of linear momentum, energy and diffusion, which govern the flow field, are solved numerically using the Galerkin finite element method, which is more economical from the computational view point. The behavior of the velocity, temperature, concentration, skin friction have been discussed for variations in the governing parameters.

2.2 FORMULATION OF THE PROBLEM

We consider the unsteady free-convection flow of an incompressible electrically conducting viscous fluid near a moving infinite flat plate in a rotating medium with velocity U_0 and rotate with angular velocity Ω as in [4]. We assume a uniform magnetic field B_0 applied in the direction of the flow fixed relative to the plate. We also assume that induced magnetic fields are negligible in comparison with the applied field. Further, we assume no applied voltage present which means no electric field present and viscous dissipation heating is absent in the energy equation. With these assumptions and those usually associated with Boussinesq approximations, the proposed governing equations are

$$\frac{\partial u'}{\partial t'} - 2\Omega' v' = \upsilon \frac{\partial^2 u'}{\partial y'^2} - \frac{\sigma B_0^2 u'}{\rho} - \frac{\upsilon u'}{K'} + g\beta(T - T_\infty) + g\beta^*(C' - C'_\infty) \tag{1}$$

$$\frac{\partial v'}{\partial t'} - 2\Omega' u' = \upsilon \frac{\partial^2 v'}{\partial y'^2} - \frac{\sigma B_0^2 v'}{\rho} - \frac{\upsilon v'}{K'} \tag{2}$$

$$\frac{\partial T}{\partial t'} = \frac{k}{\rho C_p}\left[\frac{\partial^2 T}{\partial y'^2} - \frac{1}{k}\frac{\partial q'_r}{\partial y'}\right] + \frac{\upsilon}{C_p}\left(\frac{\partial u'}{\partial y'}\right)^2 \tag{3}$$

$$\frac{\partial C'}{\partial t'} = D_m \frac{\partial^2 C'}{\partial y'^2} - k'_r(C' - C'_\infty) \tag{4}$$

Subject to the conditions

$$\begin{aligned} &u' = U_0,\ v' = 0,\ T = T_w,\ C' = C'_w \ on\ y' = 0 \\ &u' = U_0,\ v' = 0,\ T = T_\infty,\ C' = C'_\infty \ as\ y' \to \infty \end{aligned} \tag{5}$$

On introducing the dimensionless quantities

$$\left.\begin{aligned} t' &= \frac{\upsilon t}{U_0^2},\ y' = \frac{\upsilon y}{U_0},\ u' = uU_0,\ v' = vU_0,\ K' = \frac{\upsilon^2 K}{U_0^2},\ \Omega' = \frac{U_0^2\Omega}{\upsilon}, \\ Sc &= \frac{\upsilon}{D_m},\ Ec = \frac{U_0^2}{c_p(T_w - T_\infty)},\ \Pr = \frac{\mu c_p}{k},\ M^2 = \frac{\sigma B_0^2 \upsilon}{\rho U_0^2},\ k_r = \frac{k_r' \upsilon}{U_0^2}, \\ Gr &= \frac{g\beta\,\upsilon(T_w - T_\infty)}{U_0^3},\ Gc = \frac{g\beta^*\upsilon(C_w' - C_\infty')}{U_0^3},\ \theta = \frac{T - T_\infty}{T_w - T_\infty},\ C = \frac{C' - C_\infty'}{C_w' - C_\infty'} \end{aligned}\right\} \quad (6)$$

Where u, v, Velocity components; q, Complex velocity; U_0, Scale of free stream velocity; y, Coordinate; ρ, Fluid density; T, Dimensional temperature; C', Dimensional species concentration; t, Time; k, Thermal conductivity; D_m, Solutal diffusivity; C_p, Specific heat at constant pressure; β, Coefficients of volume expansion due to temperature; β^*, Coefficient of volume expansion due concentration; M^2, Hartmann number; Pr, Prandtl number; Sc, Schmidt number; Ec, Eckert number; k_r, Chemical reaction constant; K, Porosity parameter; θ, Non-dimensional temperature; C, Non - dimensional species concentration; g, Acceleration due to gravity; Gr, Grashof number; Gc, Modified Grashof number; σ, Electrical conductivity; υ, Kinematic coefficient of viscosity; Ω, Angular velocity; B_0, Magnetic field strength; q_r, Radiative flux vector;

Subscripts: w, Wall condition; ∞, Free stream condition.

In view of the above non dimensional variables, the basic field equations (1), (2) and (4), can be expressed in non dimensional form as

$$\frac{\partial u}{\partial t} - 2\Omega v = \frac{\partial^2 u}{\partial y^2} - M^2 u - \frac{u}{K} + Gr\theta + GcC \quad (7)$$

$$\frac{\partial v}{\partial t} - 2\Omega u = \frac{\partial^2 v}{\partial y^2} - M^2 v - \frac{v}{K} \quad (8)$$

$$\frac{\partial C}{\partial t} = \frac{1}{Sc}\frac{\partial^2 C}{\partial y^2} - k_r C \quad (9)$$

We now find it convenient to combine equations (7) and (8) into a single equation. We multiply equation (8) by i and add the resultant to equation (7) to obtain

$$\frac{\partial q}{\partial t}+\left(2i\Omega+M^2+\frac{1}{K}\right)q=\frac{\partial^2 q}{\partial y^2}+Gr\theta+GcC \tag{10}$$

$q=u+iv$ *and* $i=\sqrt{-1}$.

By using Rosseland approximation, the radiative heat flux q_r' is given by

$$q_r'=-\frac{4\sigma^*}{3\alpha}\frac{\partial T^4}{\partial y'} \tag{11}$$

Where σ^*-the Stefan-Boltzmann constant and α - the mean absorption coefficient. It should be noted that by using Rosseland approximation, the present analysis is limited to optically thick fluids. If temperature differences within the flow are sufficient, small, then equation (11) can be linearised by expanding T^4 in the Taylor series about T_∞, which after neglecting higher order terms take the form

$$T^4\cong 4T_\infty^3T-3T_\infty^4 \tag{12}$$

In view of equations (6), (11) and (12), equation (3) reduces to

$$\frac{\partial\theta}{\partial t}=\left(\frac{1+N}{\Pr}\right)\frac{\partial^2\theta}{\partial y^2}+Ec\left(\frac{\partial u}{\partial y}\right)^2 \tag{13}$$

Where $N=\dfrac{16\sigma^*T_\infty^3}{3k\alpha}$ is the radiation parameter.

The initial and boundary conditions are now

$$\left.\begin{aligned} &t\le 0: q(y,t)=\theta(y,t)=C(y,t)=0\\ &t>0:\begin{cases} q(0,t)=q_0 & \theta(0,t)=1 \quad C(0,t)=1\\ q(\infty,t)\to 0 & \theta(\infty,t)\to 0 \quad C(\infty,t)\to 0\end{cases}\end{aligned}\right\} \tag{14}$$

2.3 METHOD OF SOLUTION

By applying Galerkin finite element method for equation (10) over the element (e), $(y_j\le y\le y_k)$ is:

$$\int_{y_i}^{y_k}\left\{N^{(e)T}\left[\frac{\partial^2 q^{(e)}}{\partial y^2}-\frac{\partial q^{(e)}}{\partial t}-Rq^{(e)}+P\right]\right\}dy=0 \tag{15}$$

Where $P=(Gr)\theta+(Gc)C$, $R=2i\Omega+M^2+\frac{1}{K}$;

Integrating the first term in equation (15) by parts one obtains

$$N^{(e)T}\left\{\frac{\partial q^{(e)}}{\partial y}\right\}_{y_i}^{y_k}-\int_{y_i}^{y_k}\left\{\frac{\partial N^{(e)T}}{\partial y}\frac{\partial q^{(e)}}{\partial y}+N^{(e)T}\left(\frac{\partial q^{(e)}}{\partial t}+Rq^{(e)}-P\right)\right\}dy=0 \tag{16}$$

Neglecting the first term in equation (16), one gets:

$$\int_{y_i}^{y_k}\left\{\frac{\partial N^{(e)T}}{\partial y}\frac{\partial q^{(e)}}{\partial y}+N^{(e)T}\left(\frac{\partial q^{(e)}}{\partial t}+Rq^{(e)}-P\right)\right\}dy=0$$

Let $q^{(e)}=N^{(e)}\phi^{(e)}$ be the linear piecewise approximation solution over the element (e) $(y_i\le y\le y_k)$ where $N^{(e)}=\begin{bmatrix}N_i & N_k\end{bmatrix}$, $\phi^{(e)}=\begin{bmatrix}u_i & u_k\end{bmatrix}^T$ and $N_i=\frac{y_k-y}{y_k-y_i}$, $N_k=\frac{y-y_i}{y_k-y_i}$ **are the** basis functions. One obtains:

$$\int_{y_i}^{y_k}\left\{\begin{bmatrix}N_i'N_i' & N_i'N_k'\\ N_i'N_k' & N_k'N_k'\end{bmatrix}\begin{bmatrix}q_i\\ q_k\end{bmatrix}\right\}dy+\int_{y_i}^{y_k}\left\{\begin{bmatrix}N_iN_i & N_iN_k\\ N_iN_k & N_kN_k\end{bmatrix}\begin{bmatrix}\dot{q}_i\\ \dot{q}_k\end{bmatrix}\right\}dy+R\int_{y_i}^{y_k}\left\{\begin{bmatrix}N_iN_i & N_iN_k\\ N_iN_k & N_kN_k\end{bmatrix}\begin{bmatrix}q_i\\ q_k\end{bmatrix}\right\}dy$$

$$=P\int_{y_i}^{y_k}\begin{bmatrix}N_i\\ N_k\end{bmatrix}dy$$

Simplifying we get

$$\frac{1}{l^{(e)2}}\begin{bmatrix}1 & -1\\ -1 & 1\end{bmatrix}\begin{bmatrix}q_i\\ q_k\end{bmatrix}+\frac{1}{6}\begin{bmatrix}2 & 1\\ 1 & 2\end{bmatrix}\begin{bmatrix}\dot{q}_i\\ \dot{q}_k\end{bmatrix}+\frac{R}{6}\begin{bmatrix}2 & 1\\ 1 & 2\end{bmatrix}\begin{bmatrix}q_i\\ q_k\end{bmatrix}=\frac{P}{2}\begin{bmatrix}1\\ 1\end{bmatrix}$$

Where prime and dot denotes differentiation w.r.t y and time t respectively. Assembling **the** element equations for two consecutive elements $(y_{i-1}\le y\le y_i)$ and $(y_i\le y\le y_{i+1})$ **following** is obtained:

$$\frac{1}{l^{(e)2}}\begin{bmatrix}1 & -1 & 0\\ -1 & 2 & -1\\ 0 & -1 & 1\end{bmatrix}\begin{bmatrix}q_{i-1}\\ q_i\\ q_{i+1}\end{bmatrix}+\frac{1}{6}\begin{bmatrix}2 & 1 & 0\\ 1 & 4 & 1\\ 0 & 1 & 2\end{bmatrix}\begin{bmatrix}\dot{q}_{i-1}\\ \dot{q}_i\\ \dot{q}_{i+1}\end{bmatrix}+\frac{R}{6}\begin{bmatrix}2 & 1 & 0\\ 1 & 4 & 1\\ 0 & 1 & 2\end{bmatrix}\begin{bmatrix}q_{i-1}\\ q_i\\ q_{i+1}\end{bmatrix}=\frac{P}{2}\begin{bmatrix}1\\ 2\\ 1\end{bmatrix} \tag{17}$$

Now put row corresponding to the node i to zero, from equation (17) the difference schemes with $l^{(e)} = h$ is:

$$\frac{1}{h^2}\left[-q_{i-1} + 2q_i - q_{i+1}\right] + \frac{1}{6}\left[\dot{q}_{i-1} + 4\dot{q}_i + \dot{q}_{i+1}\right] + \frac{R}{6}\left[q_{i-1} + 4q_i + q_{i+1}\right] = P \qquad (18)$$

Applying the trapezoidal rule, following system of equations in Crank – Nicholson method are obtained:

$$A_1 q_{i-1}^{n+1} + A_2 q_i^{n+1} + A_3 q_{i+1}^{n+1} = A_4 q_{i-1}^{n} + A_5 q_i^{n} + A_6 q_{i+1}^{n} + P^* \qquad (19)$$

Now from equations (13) and (9) following equations are obtained:

$$B_1\theta_{i-1}^{n+1} + B_2\theta_i^{n+1} + B_3\theta_{i+1}^{n+1} = B_4\theta_{i-1}^{n} + B_5\theta_i^{n} + B_6\theta_{i+1}^{n} \qquad (20)$$

$$C_1 C_{i-1}^{n+1} + C_2 C_i^{n+1} + C_3 C_{i+1}^{n+1} = C_4 C_{i-1}^{n} + C_5 C_i^{n} + C_6 C_{i+1}^{n} \qquad (21)$$

Where $A_1 = 2 - 6r + Rk$, $A_2 = 8 + 12r + 4Rk$, $A_3 = 2 - 6r + Rk$,

$A_4 = 2 + 6r - Rk$, $A_5 = 8 - 12r - 4Rk$, $A_6 = 2 + 6r - Rk$,

$B_1 = 2(\mathrm{Pr}) - 6(1+N)r$, $B_2 = 8(\mathrm{Pr}) + 12(1+N)r$, $B_3 = 2(\mathrm{Pr}) - 6(1+N)r$,

$B_4 = 2(\mathrm{Pr}) + 6(1+N)r$, $B_5 = 8(\mathrm{Pr}) - 12(1+N)r$, $B_6 = 2(\mathrm{Pr}) + 6(1+N)r$,

$C_1 = 2(Sc) - 6r + k_r(Sc)k$, $C_2 = 8(Sc) + 12r + 4k_r(Sc)k$, $C_3 = 2(Sc) - 6r + k_r(Sc)k$,

$C_4 = 2(Sc) + 6r - k_r(Sc)k$, $C_5 = 8(Sc) - 12r - 4k_r(Sc)k$, $C_6 = 2(Sc) + 6r - k_r(Sc)k$,

$P^* = 12Pk = 12k(Gr)\theta + 12k(Gc)C$;

Here $r = \frac{k}{h^2}$ and h, k are mesh sizes along y – direction and time – direction respectively. Index i refers to space and j refers to the time. In the equations (19), (20) and (21), taking $i = 1(1)n$ and using boundary conditions (14), then the following system of equations are obtained:

$$A_1 X_i = B_i \quad i = 1(1)3 \qquad (22)$$

where A_is are matrices of order n and X_i, B_is are column matrices having n – components. The solutions of above system of equations are obtained by using Thomas algorithm for velocity, temperature and concentration. Also, numerical solutions for these equations are obtained by C –programme. In order to prove the convergence and stability of Galerkin finite element method, the same C –programme was run with smaller values

of h and k no significant change was observed in the values of q, θ and C. Hence the Galerkin finite element method is stable and convergent.

Skin – friction:

Knowing the velocity field, the skin - friction at the plate in the dimensionless form is given by $\tau = \left(\frac{\partial u}{\partial y}\right)_{y=0}$ (23)

2.4 DISCUSSION OF THE RESULTS

The problem of radiative heat transfer to unsteady hydromagnetic flow involving heat and mass transfer is addressed in this study. Numerical calculations have been carried out for the non-dimensional Temperature θ, Concentration C, Complex velocity (q) keeping the other parameters of the problem fixed. The solution obtained for the velocity is complex and only the real part of the complex quantity is invoked for the numerical discussion. Numerical calculations of these results are presented graphically in the figures from (1) to (13). These results show the effect of material parameters on the temperature distribution, concentration profiles, complex velocity and the skin friction at the wall. To find out the solution of this problem, we have placed an infinite vertical plate in a finite length in the flow. Hence, we solve the entire problem in a finite boundary. However, in the graphs, the y values vary from 0 to 4 and the complex velocity, temperature, and concentration tend to zero as y tends to 4. This is true for any value of y. Thus, we have considered finite length. In the present study we adopted the following default parameter values of finite element computations: $Gr = 1.0$, $Gc = 1.0$, $M = 1.0$, $K = 1.0$, $\Pr = 0.71$, $N = 1.0$, $Ec = 0.001$, $Sc = 0.22$, $k_r = 1.0$ All graphs therefore correspond to these values unless specifically indicated on the appropriate graph.

The temperature and the species concentration are coupled to the velocity via Grashof number (Gr) and Modified Grashof number (Gc) as seen in equation (10). For various values of Grashof number and Modified Grashof number on the complex velocity profiles q are plotted in figures (1) and (2). The Grashof number (Gr) signifies the relative effect of the thermal buoyancy force to the viscous hydrodynamic force in the boundary layer. As expected, it is observed that there is a rise in the velocity due to the

enhancement of thermal buoyancy force. Also, as (Gr) increases, the peak values of the velocity increases rapidly near the porous plate and then decays smoothly to the free stream velocity. The Modified Grashof number (Gc) defines the ratio of the species buoyancy force to the viscous hydrodynamic force. As expected, the fluid velocity increases and the peak value is more distinctive due to increase in the species buoyancy force. The velocity distribution attains a distinctive maximum value in the vicinity of the plate and then decreases properly to approach the free stream value. It is noticed that the velocity increases with increasing values of Modified Grashof number (Gc).

Figure (3) depicts the effect of Prandtl number on complex velocity profiles in presence of foreign species such as Mercury (Pr = 0.025), Air (Pr = 0.71), Water (Pr = 7.00) and Methanol (Pr = 11.62) are shown in figure (3). We observe that from figure (3), the complex velocity decreases with increasing of Prandtl number (Pr). Figure (8) depicts that the temperature profiles (θ) against y taking different values of Prandtl number (Pr). The thermal boundary layer thickness is greater for fluids with small Prandtl number. The reason is that smaller values of Prandtl number are equivalent to increasing thermal conductivity and therefore heat is able to diffuse away from the heated surface more rapidly than for higher values of (Pr). The effects of the thermal radiation parameter (N) on the complex velocity and temperature profiles in the boundary layer are illustrated in figures (4) and (9) respectively. Increasing the thermal radiation parameter (N) produces significant increase in the thermal condition of the fluid and its thermal boundary layer. This increase in the fluid temperature induces more flow in the boundary layer causing the velocity of the fluid there to increase. The nature of complex velocity profiles in presence of foreign species such as Hydrogen (Sc = 0.22), Helium (Sc = 0.30), Water vapour (Sc = 0.60) and Oxygen (Sc = 0.66) are shown in figure (6). The flow field suffers a decrease in complex velocity at all points in presence of heavier diffusing species.

Figure (11) shows the concentration field due to variation in Schmidt number (Sc) for the gasses Hydrogen, Helium, Water–vapour and Oxygen. It is observed that concentration field is steadily for Hydrogen and falls rapidly for Water–vapour and Oxygen in comparison to Helium. Thus Hydrogen can be used for maintaining effective concentration field and Helium can be used for maintaining normal concentration field.

Figures (5) and (10) display the effects of the Eckert number on the complex velocity and temperature profiles. For the parametric values used to obtain these figures, it is seen that increasing the Eckert number (Ec), leads to both the complex velocity and temperature profiles with no changes in the momentum and thermal boundary layer thicknesses.

Figures (7) and (12) display the effects of the chemical reaction parameter (k_r) on the complex velocity and concentration profiles, respectively. As expected, the presence of the chemical reaction significantly affects the concentration profiles as well as the velocity profiles. It should be mentioned that the studied case is for a destructive chemical reaction(k_r). In fact, as chemical reaction(k_r) increases, the considerable reduction in the velocity profiles is predicted, and the presence of the peak indicates that the maximum value of the velocity occurs in the body of the fluid close to the surface but not at the surface. Also, with an increase in the chemical reaction parameter, the concentration decreases. It is evident that the increase in the chemical reaction (k_r) significantly alters the concentration boundary layer thickness but does not alter the momentum boundary layers. The effect of rotation parameter (Ω) on complex velocity profiles is as shown in the figure (13). Form this figure, we observe that the velocity profiles increases with increasing values of rotation parameter.

The profiles for skin – friction (τ) due to complex velocity under the effects of Grashof number (Gr), Modified Grashof number (Gc), Magnetic number (M), Permeability parameter(K), Prandtl number(Pr), Thermal radiation parameter (N) Eckert number (Ec), Schmidt number (Sc), and Chemical reaction (k_r) are presented in the table 1. We observed that an increase in the Prandtl number or Schmidt number or Eckert number or chemical reaction or magnetic parameter leads to decrease in the value of skin-friction coefficient whereas an increase in the Grashof number or Modified Grashof number or radiation parameter or permeability parameter leads to increase in the value of skin-friction coefficient.

Table 1: Skin – friction coefficient (τ)

Gr	Gc	M	K	Pr	N	Ec	Sc	k_r	τ
1.0	1.0	1.0	1.0	0.71	1.0	0.001	0.22	1.0	1.2265
2.0	1.0	1.0	1.0	0.71	1.0	0.001	0.22	1.0	2.4398
1.0	2.0	1.0	1.0	0.71	1.0	0.001	0.22	1.0	2.4215
1.0	1.0	2.0	1.0	0.71	1.0	0.001	0.22	1.0	1.1684
1.0	1.0	1.0	2.0	0.71	1.0	0.001	0.22	1.0	1.5307
1.0	1.0	1.0	1.0	7.0	1.0	0.001	0.22	1.0	1.0568
1.0	1.0	1.0	1.0	0.71	2.0	0.001	0.22	1.0	1.3602
1.0	1.0	1.0	1.0	0.71	1.0	0.01	0.22	1.0	1.2015
1.0	1.0	1.0	1.0	0.71	1.0	0.001	0.30	1.0	1.0026
1.0	1.0	1.0	1.0	0.71	1.0	0.001	0.22	2.0	1.1968

OBSERVATIONS:

In this chapter we have examined the governing equations for unsteady hydro magnetic natural convection heat and mass transfer flow of a rotating Boussinesq fluid past a vertical porous plate in the presence of radiative heat transfer. Employing Finite element technique, the leading equations are solved numerically in the complex plane. We present results to illustrate the flow characteristics for the velocity and temperature fields as well as the skin – friction show how the flow fields are influenced by the material parameters of the flow problem.

1. It is observed that the complex velocity (q) of the fluid increases with the increasing of parameters Gr, Gc, N, Ec and decreases with the increasing of parameters Pr, Sc and k_r.

2. The fluid temperature (θ) increases with the increasing of N and Ec and decreases with the increasing of Pr.

3. The Concentration of the fluid decreases with the increasing of k_r and Sc.

4. From table (1) it is concluded that the magnitude of shearing stress τ increases as the increasing values of Gr, Gc, N, and this behavior is found just reverse with the increasing of Pr, Sc, Ec, and k_r.

2.5 REFFERENCES

[1] Agarwal H.L., Ram P. C., and Singh V., effects of Hall currents on the hydro-magnetic free convection with mass transfer in a rotating fluid, Astrophys.space sci.,100,297-283 (1984).

[2] Azzam G.E.A., radiation effects on the MHD Mixed Free-Fixed convection Flow past a semi-infinite moving vertical plate for high temperature differences, Phys. Scripta.,66, 71-76 (2002).

[3] Bestman A.R., Free Convection Heat Transfer to Steady Radiating Non-Newtonian MHD Flow Past a Vertical Porous Plate, *Int. J. Numer. Methods Eng.*, 21, 899 – 908 (1985).

[4] Bestman A.R., and Adjepong S.K., Unsteady Hydro-magnetic Free-convection Flow with Radiative heat Transfer in a Rotating Fluid Astrophys.space sci.,143,217-224 (1998).

[5] Chamkha A. J., Thermal Radiation and Buoyancy Effects on Hydro-magnetic Flow Over an Accelerating Permeable Surface with Heat Source or Sink, *Int. J. Eng. Sci.*, 38,1699 – 1712 (2000).

[6] Chamkha A.J., Unsteady MHD Convective Heat and Mass Transfer Past a Semi-infinite Vertical Permeable Moving Plate with Heat Absorption, *Int. J. Eng. Sci.*, 42, 217 – 230 (2004).

[7] Cookey C. I., A. Ogulu and Omubo-Pepple V. B., Influence of Viscous Dissipation And Radiation on Unsteady MHD Free-convection Flow Past an Infinite Heated Vertical Plate in a Porous Medium with Time Dependent Suction, *Int. J. Heat Mass Transfer.*, 46, 2305 – 2311 (2003).

[8] E. M. E. Elbarbary and N. S. Elgazery, Chebyshev Finite Difference Method for the Effect of Variable Viscosity on Magneto Micro-Polar Fluid Flow with Radiation, *Mass Transfer Int. Comm. Heat.*, 31(3), 409-419 (2004).

[9] Gireesh kumar J, Satyanarayana P.V. and Ramakrishna, effects of chemical reaction and mass transfer on MHD unsteady Free-convection Flow Past an Infinite Vertical Plate with constant Suction and heat sink, Ultra Science, 21(3), 639-650(2009).

[10] Helmy K.A., Unsteady Free Convection Flow Past a Vertical Porous Plate, *ZAAM. Z. Agnew. Mech.*, 78(4), 255-270 (1998).

[11] Ibrahim F. S., Hassanein I. A. and Bakr A. A., Unsteady Magneto Hydro-dynamic Micro-polar Fluid Flow and Heat Transfer over a Vertical Porous Medium in the Presence of Thermal and Mass Diffusion with Constant Heat Source, *Canada. J. Phys.*, 82, 775 – 790 (2004).

[12] Jha B. K., MHD Free-Convection and Mass Transfer Flow through a Porous Medium, *Astrophys. Space Sci.*, 175, 283-289 (1991).

[13] Kandasamy R., Periasamy K. and Prabhu K.K.S., Effects of Chemical Reaction Heat and Mass Transfer Along a Wedge with Heat Source and Convection in the Presence of Suction or Injection, *Int. J. Heat Mass Transfer.*, 48, 1288 – 1394 (2005).

[14] Kesavaiah D.Ch., Satyanarayana P.V.and Venkataramana S., Effects of the chemical reaction and radiation absorption on an Unsteady MHD Convective Heat and mass Transfer flow Past a Semi-infinite Vertical permeable Moving Plate embedded in a porous medium with heat Source and Suction, Int. J. of Appl. Math and Mech. 7(1), 52-69(2011).

[15] Kim Y.J., Unsteady MHD Convective Heat Transfer Past a Semi-infinite Vertical Porous Moving Plate with Variable Suction, *Int. J. Eng. Sci.*, 38, 833 – 845 (2000).

[16] Muthucumaraswamy R. and Ganesan P., Natural Convection on a Moving Isothermal Vertical Plate with Chemical Reaction, *J. Eng. Phys. Thermophys.*, 71 (1), (2002).

[17] A. Ogulu and C.I. Cookey, MHD Free-Convection and Mass Transfer Flow with Radiative Heat Transfer, *Model. Measure. Contr.*, B 70, (1-2), 31-37 (2001).

[18] Ogulu A. and Prakash J., Heat Transfer to Unsteady Magneto-hydrodynamic Flow Past an Infinite Moving Vertical Plate with Variable Suction, *Physica Scripta.*, 74, 232 (2006).

[19] Prakash J., Ogulu A. and Zhandire E., MHD free convection and mass transfer flow of a micro-polar thermally radiating and reacting fluid with time dependent suction, *Indian J Pure and Appl phys.*, 46, 679 (2008).

[20] Pantokratoras A., Non-Darcian Forced Convection Heat Transfer over a Flat Plate in a Porous Medium with Variable Viscosity and Variable Prandtl number, *J. Porous Media*, 10, 201-208 (2007).

[21] Sudheer Babu M. and Satyanarayana P.V., Effects of chemical reaction and radiation absorption on free convection flow through porous medium with variable suction in the presence of uniform magnetic field, J.P.Journal of Heat and Mass transfer,3, 219-234 (2009).

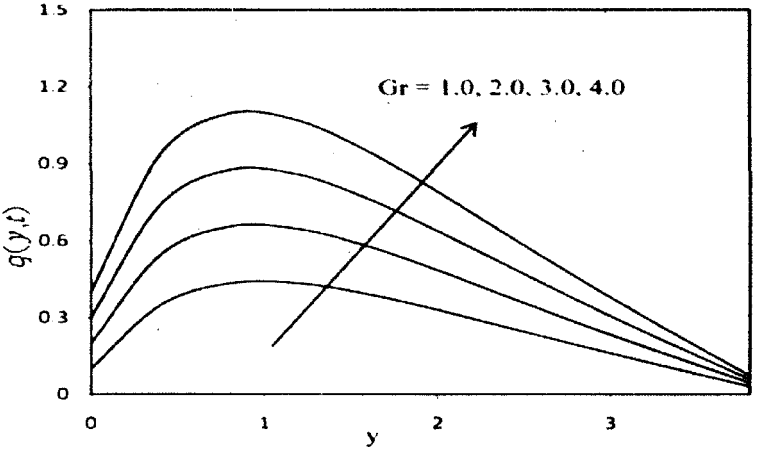

Figure 1. Velocity profiles for different values of *Gr*

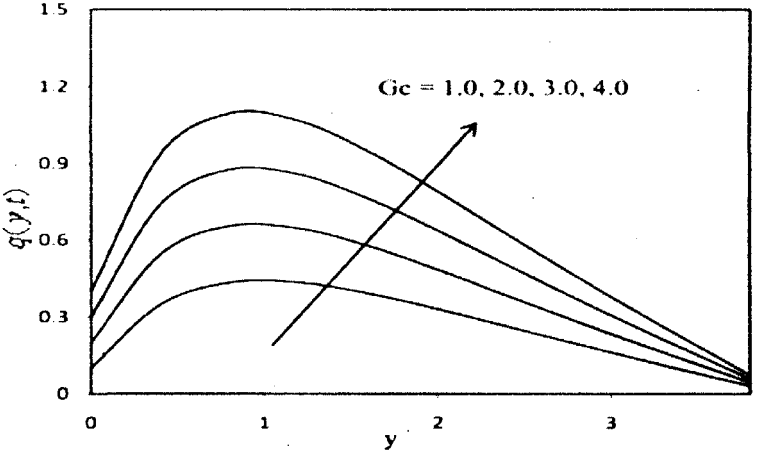

Figure 2. Velocity profiles for different values of *Gc*

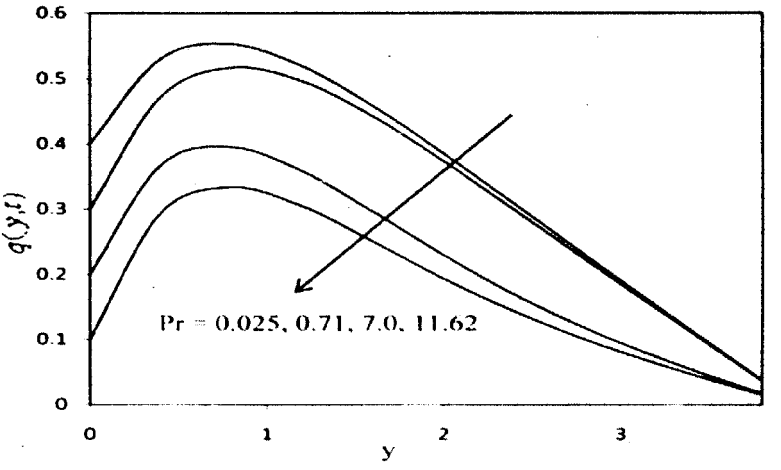

Figure 3. Velocity profiles for different values of Pr

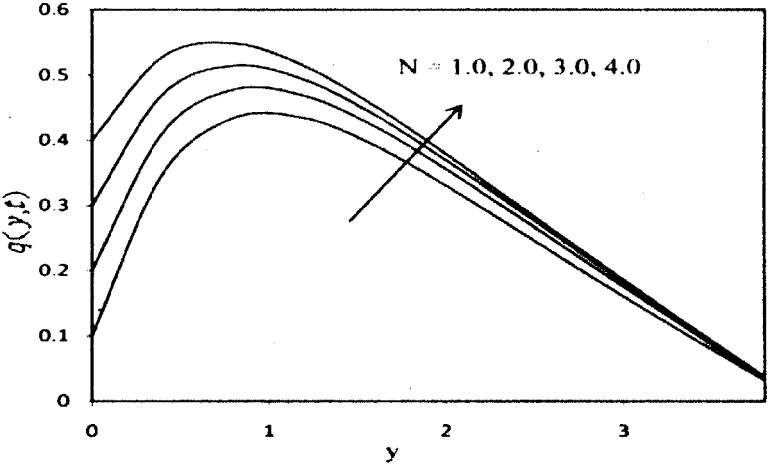

Figure 4. Velocity profiles for different values of N

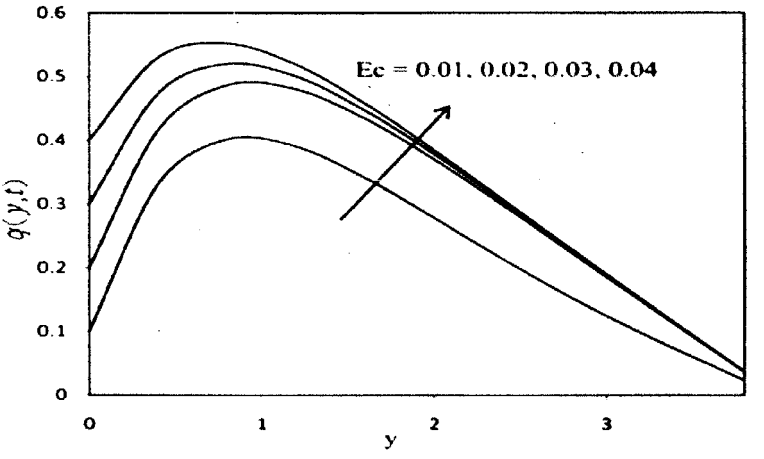

Figure 5. Velocity profiles for different values of *Ec*

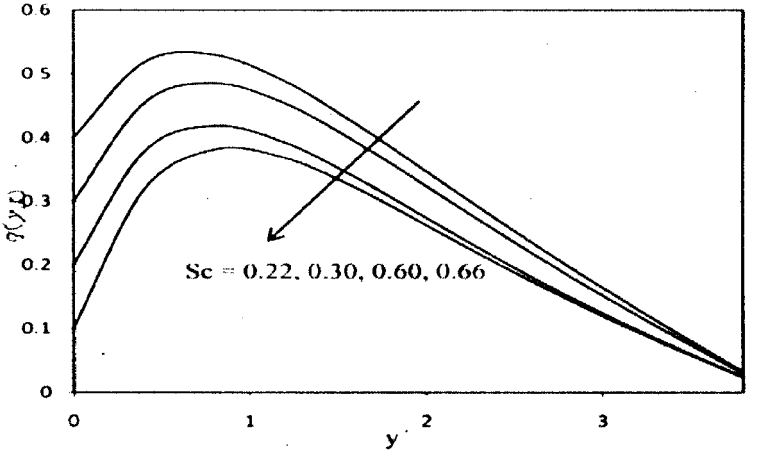

Figure 6. Velocity profiles for different values of *Sc*

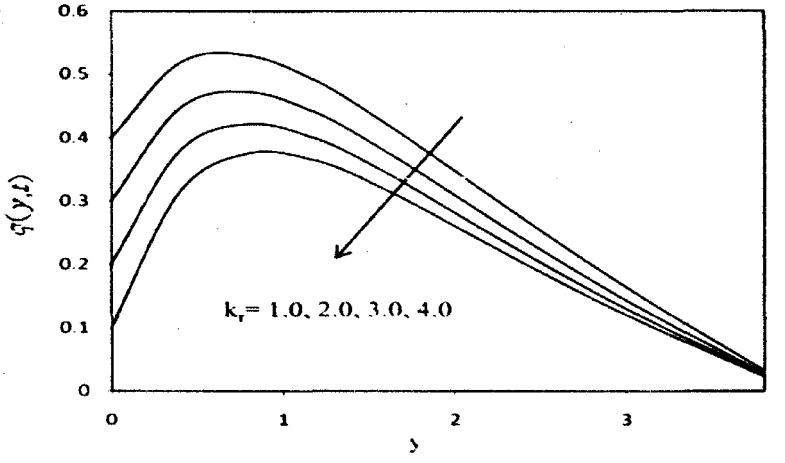

Figure 7. Velocity profiles for different values of k_r

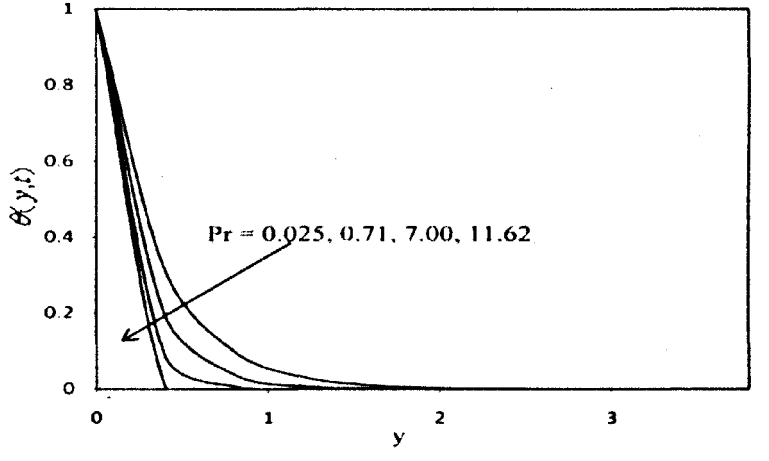

Figure 8. Temperature profiles for different values of Pr

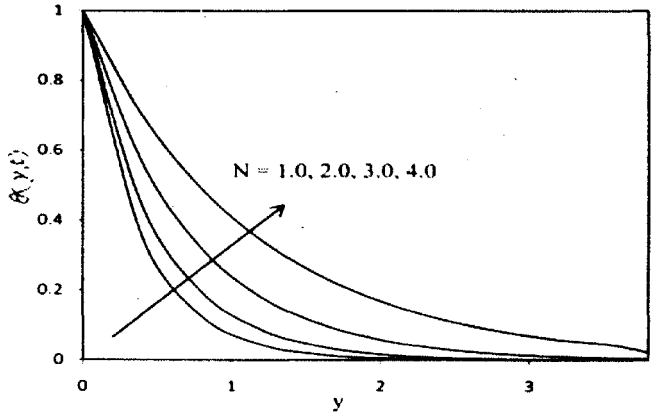

Figure 9. Temperature profiles for different values of N

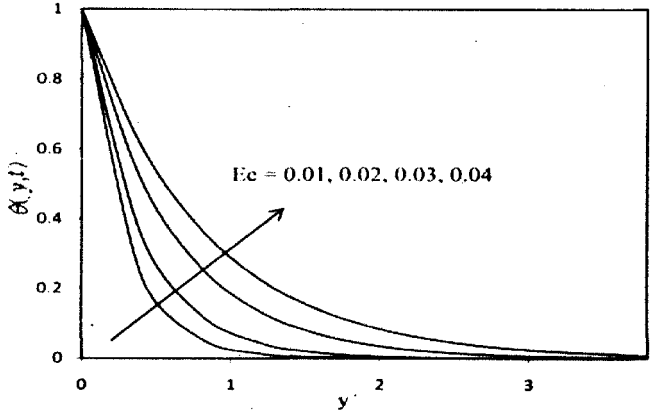

Figure 10. Temperature profiles for different values of Ec

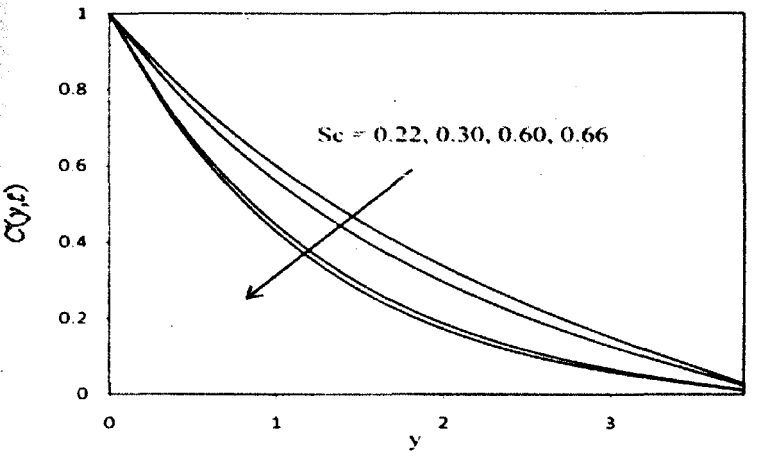

Figure 11. Concentration profiles for different values of Sc

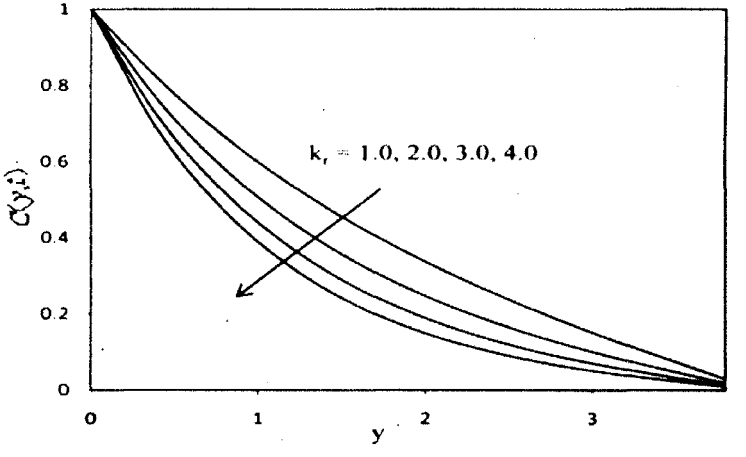

Figure 12. Concentration profiles for different values of k_r

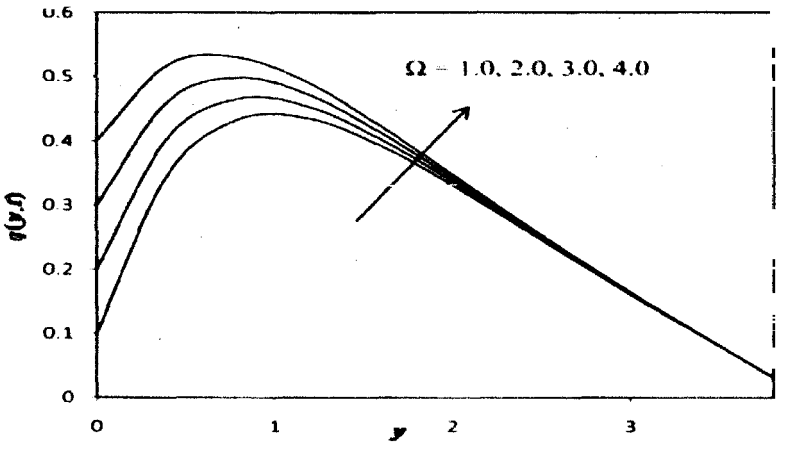

Figure 13. Velocity profiles for different values of Ω